DOI: 10.3901/CJME.2016.0418.054, available online at www.springerlink.com; www.cjmenet.com

Synthesized Multi-station Tribo-test System for Bio-tribological Evaluation in Vitro

WU Tonghai[1, 2, *], DU Ying[1], LI Yang[1], WANG Shuo[1], and ZHANG Zhinan[3]

1 *Key Laboratory for Modern Design and Rotor-Bearing System of Ministry of Education, Xi'an Jiaotong University, Xi'an, 710049, China*
2 *State Key Laboratory of Mechanical Transmissions, Chongqing University, Chongqing, 400044, China*
3 *School of Mechanical Engineering, Shanghai Jiao Tong University, Shanghai, 200240, China*

Received August 31, 2015; revised March 30, 2016; accepted April 18, 2016

Abstract: Tribological tests play an important role on the evaluation of long-term bio-tribological performances of prosthetic materials for commercial fabrication. Those tests focus on the motion simulation of a real joint in vitro with only normal loads and constant velocities, which are far from the real friction behavior of human joints characterized with variable loads and multiple directions. In order to accurately obtain the bio-tribological performances of artificial joint materials, a tribological tester with a miniature four-station tribological system is proposed with four distinctive features. Firstly, comparability and repeatability of a test are ensured by four equal stations of the tester. Secondly, cross-linked scratch between tribo-pairs of human joints can be simulated by using a gear-rack meshing mechanism to produce composite motions. With this mechanism, the friction tracks can be designed by varying reciprocating and rotating speeds. Thirdly, variable loading system is realized by using a ball-screw mechanism driven by a stepper motor, by which loads under different gaits during walking are simulated. Fourthly, dynamic friction force and normal load can be measured simultaneously. The verifications of the performances of the developed tester show that the variable frictional tracks can produce different wear debris compared with one-directional tracks, and the accuracy of loading and friction force is within ±5%. Thus the high consistency among different stations can be obtained. Practically, the proposed tester system could provide more comprehensive and accurate bio-tribological evaluations for prosthetic materials.

Keywords: artificial joint, multi-station, tribological tester, bio-tribology, testing system

1 Introduction

Arthroplasty is a reliable method for treating joint diseases[1]. When human joints are damaged or diseased, they could be replaced by an artificial joint using a wide range of materials[2]. The bio-tribological performances of the contact pairs play a significant role on the long-term performances of the prostheses[3–4], where the main problem is the wear of orthopedic materials[5]. Consequently, a bio-tribology testing system on material evaluations is appealing increasing interests to higher demands of closeness to real working conditions of human joints.

Bio-tribological tests can be divided into two types, in vivo and in vitro. In-vivo studies, which can provide information under real physiological conditions, have been performed to investigate the friction behavior of artificial joints[6–7]. However, these processes are complex and the results are diversiform[8], so, it is very hard to get a unified conclusion or standard data. In comparison, in vitro studies are feasible for the evaluations on the material of artificial joints with controllable conditions and accessible information[9–10]. Additionally, the results have the characteristics of good regularity, comparability and repeatability. Therefore, the tribo-tests of these sliding partners in vitro can take place of in vivo tests to simulate friction behaviors and conditions of human joints[11]. However, there are large differences between the test results and clinical data[12], because of complicated motion features and working conditions of human joints[13].

As motion simulation becoming one of the most critical factors to imitate performances of a real joint, many researchers were focusing on the development of the multi-track tester. Hip simulator, which was capable to perform spatial motions of a real joint, was developed with a special mechanical mechanism by Leeds university[14]. Full simulation tests used a real product to examine its

* Corresponding author. E-mail: wt-h@163.com
Supported by Funding of State Key Laboratory of Mechanical Transmissions, Chongqing University, China(Grant No. SKLMT-KFKT-201504), National Natural Science Foundation of China(Grant No. 51275381), and Science and Technology Planning Project of Shaanxi Province, China(Grant No. 2012GY2-37)

performances under similar conditions, such as multi-dimensional motion, lubrication, sliding friction, and so forth. However, such systems were designed for an entire artificial part and mostly focusing on the wear performances of fabricated parts. Generally, material-based evaluation, which should be considered beforehand when manufacturing a product, requires basic testing with specified movements and conditions, such as planar testers, and exhibits superiority over a full simulator[15]. For a normal planar tester, such as HUT-RPF[16], COMOC-POD [17], etc., the motion between the two samples was simple and the direction of the friction was constant. Additionally, the simulated motion was also simple and easy to analyze friction and wear properties. In 1976, Charnley first presented an interesting multi-directional motion pin-on-disk device[18]. Subsequently, Saikko found that, compared with a normal pin-on-disk tester, the morphology of wear debris from a multi-directional pin-on-disk tester was much closer to the particles produced from an artificial joint in practical applications[19]. The reason was that the friction factors and wear rates of materials for artificial joints were largely depended on the kinetic characteristics of tribo-pairs[20–22].

Variable environmental parameters, including loads, speeds, motions etc., are fundamental for the evaluation of prosthetic materials. The contact stresses of human joints are constantly changed with varied walking conditions. Therefore, the movement and stress states of the joint have been taken into account when evaluating materials of artificial joints by tribo-testers. Correspondingly, multi-directional and variable loads are necessary for basic tests of prosthetic materials. Saikko developed a Circularly Translating Pin-on-disk Device(CTPOD), which showed similar wear rates and wear mechanisms to those observed in retrieved polyethylene acetabular cups[23]. However, both the loads and the rotate speeds were adopted constantly during the tests. Similarly, a planar tester, developed by Harbin Institute of Technology, was capable of all-the-journey gradually-changing-direction as well as the constant velocity and the normal load[24].

Repeatability is also critical in a tribological testing. To maintain highly similar working conditions for different tribo-tests, multi-stations with one control unit were adopted in some tribo-testers. By doing this, these copied stations worked synchronously under the same environment. However, such designs with synchronous stations were suitable for copied tests, but they were not for comparative examinations among different samples, in which some variables generally varied with others were fixed.

To cope with the requirements of comprehensive bio-tribological tests, a tribo-tester is designed stressing on friction path planning, independent multiple working stations, automatically varied loads and movement rates. Specifically, four independent stations are adopted for the synchronous and independent tests to perform comparability and repeatability of a test evaluation. A gear-rack meshing mechanism is used to produce a multi-directional friction by combining simple reciprocating and rotational motion of lower and upper samples, respectively. Variable normal loads are accomplished by digital control. Furthermore, specified experiments are carried out to inspect the performances of the constructed tester.

2 Design of the Bio-tribological Tester

With respect to the versatility and feasibility, a planar pin-on-disk was adopted as the basic contact method commonly recommended by references. An upper cylinder sample pin was fixed in a pin holder; on the contrary, the lower flake sample was fixed in a rectangle container filled with the tissue fluid as the lubricant. Reciprocation was adopted on account of simulating similar movements to human joints.

As shown in Fig. 1, a slider fixed on a ball-screw is supported by two parallel slider-ways.

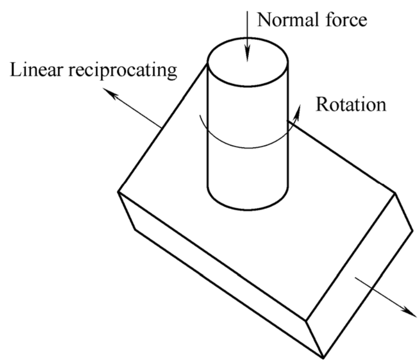

Fig. 1. Principle of the composite motion

The reciprocation of the slider was driven by a stepper motor. To realize accurate location of the slider, an electronic cursor was equipped, where feedbacks were obtained to adjust the motor controller. In practical, a disk, which was fixed with a slider, was regarded as the target sample container. The disk was moving under a controllable distance and speed.

In the rest of this chart, we mainly focus on the design of multi-directional friction paths, high precise loading system, and independent multi-stations.

2.1 Design on multi-directional friction paths

Generally, the multi-directional friction of two contact parts can be realized using the motion synthesis of two directional independent motions. However, real joint moves within a small scale, thus a simplified dependent motion can be adopted in a simulation. Therefore, a linkage mechanism was considered by which the upper and lower specimens can move dependently.

A gear-rack transmission was used with a rack fixed on the disk carrier and a gear fixed on the pin holder, shown in Fig. 2. When the disk reciprocated, the pin was driven by the gear-rack transmission and twisted within a certain angle. Consequently, a synthesis motion can be achieved by the two dependent movements of the upper and the lower specimens.

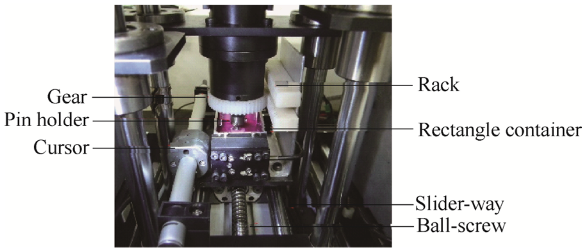

Fig. 2. Image of gear-rack meshing mechanism

To qualitatively investigate the tracks by this friction, theoretical computations were carried out afterwards.

2.1.1 Relative motion model of the contact surfaces

The relative motion between the pin and the disk produces a complex orbit as a human joint does. Therefore, the relative motion path, as well as wear tracks, was studied mathematically with a simplified model, shown in Fig. 3.

A coordinate system was established with the center O' at the center of the disk. The synthesis motion can be equivalent to the movement of the pin on the standstill disk. Specifically, the pin's center O moved to a new center O_1, and the reference point K on the surface of the pin rotated to a new point K_1. Correspondingly, the displacement and the rotate angle were X_0 and γ, respectively.

In the design, the pitch diameter is 45 mm, and the modules of both the selected gear and rack are 1. Thus the coordinate of the point K_1 can be computed as

$$x = X_0 - \rho\sin\left(\frac{2X_0}{45}+\theta\right), \tag{1}$$

$$y = \rho\cos\left(\frac{2X_0}{45}+\theta\right). \tag{2}$$

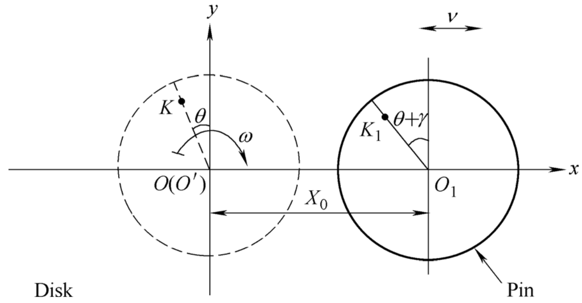

Fig. 3. Coordinate system with the center O' of the disk as the original point

v—Reciprocation rate of the disk, mm/s;
n—Gear's rotation rate, r/min;
d—Pitch diameter of gear, mm;
ω—Rotational angular velocity of the gear, rad/s;
X_0—Relative displacement of the disk and the pin during the time t; and $X_0\in[-S/2, S/2]$, where S is the reciprocating stroke that user inputs.

The relationship between S and γ can be obtained from the above formulas.

2.1.2 Wear tracks

To investigate the tracks of the pin moving on the disk, tracks of different representative points of the pin's surface were calculated. Total 48 points were selected with the consideration of their locations of 8 phase angles and 6 radiuses. For a fixed reciprocating stroke, tracks of the 48 points were plotted in the same coordinate system as shown in Fig. 4.

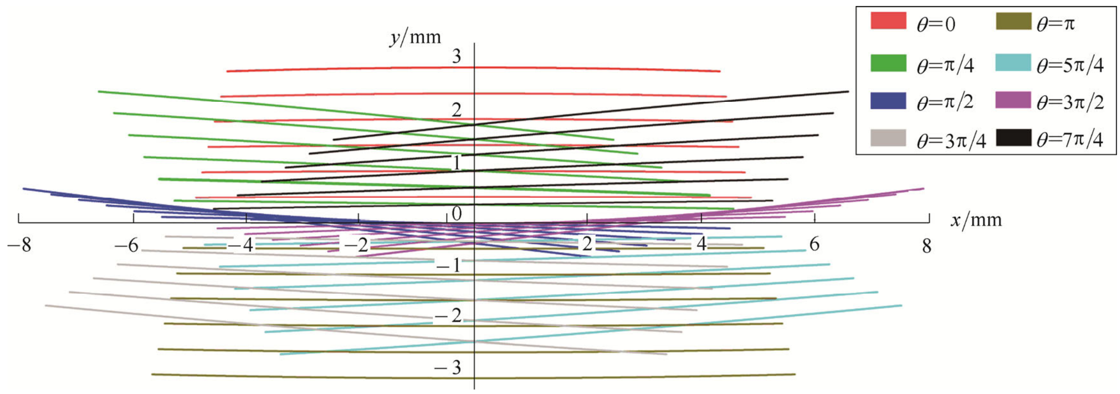

Fig. 4. Multi-directional and cross-linked tracks of different points in different distances(ρ) under different phase angles

It is observed that tracks of different points are highly cross-linked. This implicates that the moving direction of the points in the pin surface changes constantly during the movements. And points at different phase angles produce crossed tracks even within a small twist angle. Consequently, multi-directional motion between the two specimens can be obtained with the above design.

2.2 Working station design

To facilitate a comparative and repeatable evaluation, four equal stations were designed, providing the synchronous and independent tests. Each station mainly consisted of the loading components and the reciprocating components. The sketch of the station is shown in Fig. 5.

2.2.1 Variable loading system

Variable and precise loading are fundamental for simulating human joints on walking conditions. Practically, the load of the articular surface from a moving person is not a stable value. Therefore, spectrum loads were adopted in the current design to imitate the loading condition of human joints.

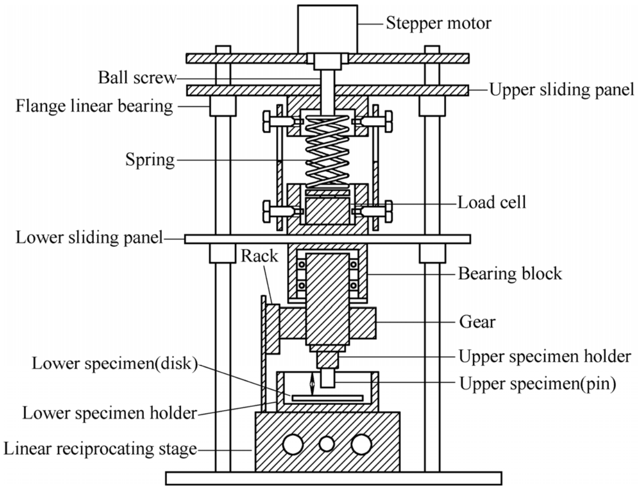

Fig. 5. Sketch of individual station

The strategy of the loading system is shown in Fig. 5. A ball-screw mechanism driven by a step-motor was adopted to produce vertical loads, which was transduced from the upper specimen to the lower one. Generally, the surface of a bio-sample will inevitably have fluctuations with a rigid load.

A real-time feedback from a load cell was required to tell the derivation from the pre-set value. Afterwards, this deflection would be modified by the executive loading mechanism. Meanwhile, the nut of the ball-screw was connected with the holder of the load cell by flexible connecting with pull rod and pressure-bearing spring. The precision of the load can be identified with its resolution computed as

$$A = \frac{P_{\mathrm{h}} K \alpha}{360}, \tag{3}$$

where A—Resolution of load, N;

P_{h}—Lead of ball screw, mm;

K—Stiffness coefficient of spring, N/mm;

α—Step angle of the loading motor.

The resolution of the load is 0.008 7 N according to the parameters of selected parts(K=27.95 N/mm, P_h=1mm, α=0.112 5°). Considering the weight of the bearing block and the gear, the range of the loading force is from 14.5N to 200N.

2.2.2 Reciprocating movement

The lower specimen is fixed in the lower specimen holder, which is installed on the two linear slide rails, shown in Fig. 6. The friction force sensor holder is fixed in the linear reciprocating stage. The stepper motor drives the rotation of the ball screw, which drives the linear reciprocating stage moving back and forth. At the same time, the lower specimen moves back and forth with different speeds.

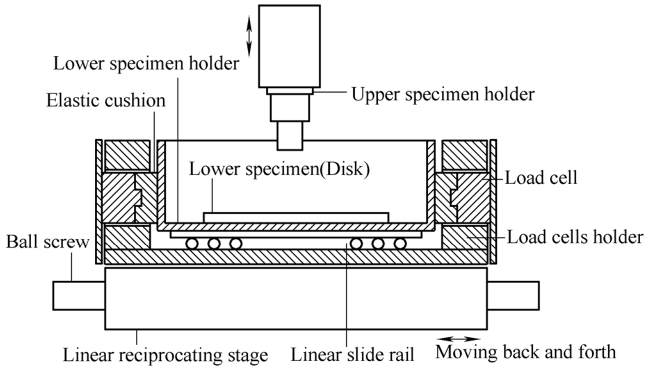

Fig. 6. Sketch of the reciprocating components

2.2.3 Dynamic friction coefficient measurements

Dynamic friction coefficient is used to characterize the tribological performances of object specimens. To do this, the friction force between the upper and the lower samples is precisely measured during the reciprocation. As shown in Fig. 7, the lower specimen holder is fixed on a linear slider that separates the sample holder from the linear reciprocating stage with extremely lower friction rolling bearings. This design excludes the additional friction force from the object. Two load cells were arranged at the two end sides of the surfaces of the lower specimen holder respectively, and contacted with the container surfaces under preloads. The preload can be adjusted by screws to ensure that the load cells works in their linear range.

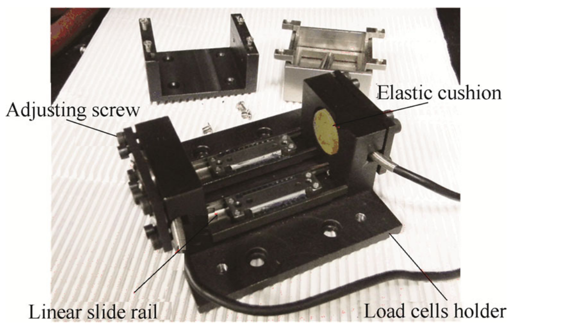

Fig. 7. Two linear slide rails were arranged in load cells holder

To avoid a rigid contact of the load cell and the container, elastic cushions were applied between the contact surfaces. By doing this, the friction force yielded between the tribo-pairs will be transmitted directly to the load cells, which is reflected by signals of the sensor.

A force analysis diagram of the lower specimen is shown in Fig. 8.

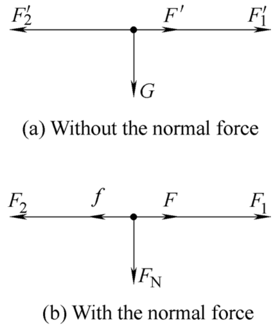

Fig. 8. Force conditions of the lower specimen

where F_1'—Force of the left sensor;
F_2'—Force of the right sensor;
F'—Friction force between the linear slide rail and the load cell holder;
G—Weight of the lower specimen and its holder;
F_1—Force of the left sensor;
F_2—Force of the right sensor;
F—Friction force between the linear slide rail and the load cell holder;
F_N—Normal force;
f—Friction force.

Before loading, as the force analysis diagram is shown in Fig. 8(a), the following equation can be given as

$$F_1' + F' = F_2'. \tag{4}$$

The friction coefficient of the slide-ways is extremely low ($\mu' = 0.01$) that the friction force can be ignored in this study, which is introduced by the two slide ways and the weight of the lower specimen and its holder. So the equation can be simplified as

$$F_1' = F_2', \tag{5}$$

where $F=kV+b$;
F—Loads of the sensor, N;
V—Output voltage of the sensor, V;
K, b—Coefficients of this linear relationship.

So, we have

$$k_1 V_1' + b_1 = k_2 V_2' + b_2, \tag{6}$$

where V_1'—Output voltage of the left force sensor at the beginning of the tests;
V_2'—Output voltage of the right force sensor at the beginning of the tests.

Under loading, in the case that the linear reciprocating stage moves to the right, a force analysis diagram is shown in Fig. 8(b). The following equation can be given as

$$f + F_2 = F + F_1, \tag{7}$$

$$f = F + k_1 V_1 + b_1 - k_2 V_2 - b_2. \tag{8}$$

Combining Eqs. (8) with Eqs. (6), we have

$$f = F + k_1 (V_1 - V_1') + k_2 (V_2' - V_2), \tag{9}$$

where V_1—Output voltage of the left force sensor with the stage moving to the right;
V_2—Output voltage of the right force sensor with the stage moving to the right.

And when the linear reciprocating stage moves to the left, the force of the lower specimen is

$$f = F + k_1 (V_1' - V_1) + k_2 (V_2 - V_2'). \tag{10}$$

The friction force between the samples can be obtained by combining Eq. (9) with Eq. (10), given as

$$f = F + k_1 |V_1' - V_1| + k_2 |V_2 - V_2'|. \tag{11}$$

So, we have

$$f = F + k_1 \Delta_1 + k_2 \Delta_2, \tag{12}$$

where Δ_1, Δ_2—Output voltage variations of the left force sensor and the right force sensor, respectively.

Since $f = \mu F_N$, we have

$$\mu = \frac{F}{F_N} + \frac{k_1 \Delta_1 + k_2 \Delta_2}{F_N}, \tag{13}$$

where F/F_N—Friction coefficient of the slide-ways, and the value is 0.01, as previously mentioned.

By Eq. (13), the dynamic friction coefficient can be obtained with the output voltages of the two sensors.

2.3 Flow chart of data acquisition and motion control

Data acquisition system is responsible for signal collection, including normal loads, friction forces, and location of sliders, shown in Fig. 9.

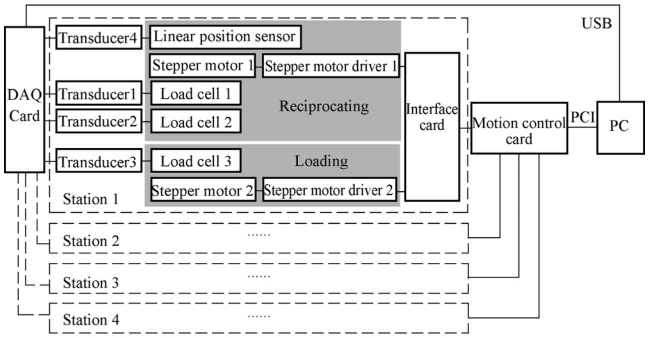

Fig. 9. Schematic of Data acquisition and Motion control

A motion control card was used to control the motion of stepper motors. A computer was applied to manage the user interfaces and monitor the testing system in real-time.

The reciprocating motion schematic is presented in Fig. 10. The input reciprocating stroke S was converted to the voltages of limiting positions(V_A, V_B). The input testing time(T) determined the execution of the main program circulation, where a timer recorded the elapsed time (t_i), and then a comparison was conducted between the input time and the elapsed time during the test. When time was up, the reciprocating stepper motor would be stopped and the loading system would be upraised, indicated that the test was going to be finished. The range of the reciprocating frequency is 0.05–1.25 Hz, which meets the accuracy requirements described in ISO 14243–1: 2009. In other words, the testing frequency should be 1+0.1Hz. Additionally, the range of the reciprocating velocity is 0–10 mm/s.

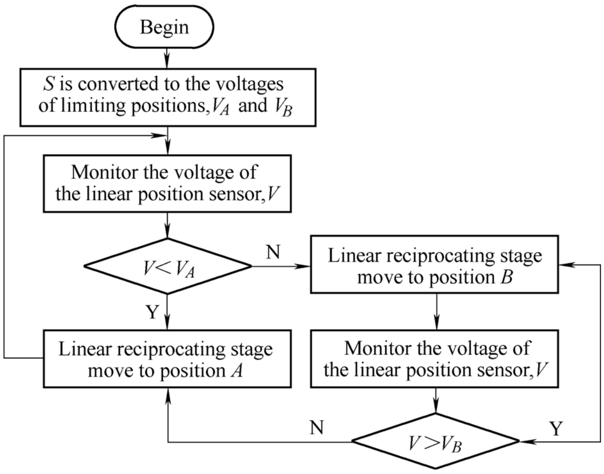

Fig. 10. Schematic of the reciprocating motion

2.4 Implementation of the tribo-test system

The testing system was built according to the above design. As shown in Fig. 11, four independent working stations are employed in this system, in order to obtain the comparability and repeatability by conducting the experiments simultaneously.

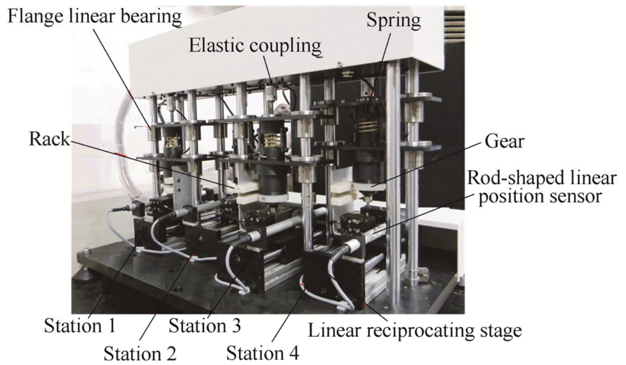

Fig. 11. Tribo-test system with four-station

3 Validation of the Tribo-test System

Experiments were designed to evaluate the performances of the newly-designed tester. Specifically, three performances were examined, including multi-directional friction tracks, the consistency of four stations, and the accuracy of the loading function.

The first test on friction tracks was performed with a bone-like material, magnesium alloy. The density and elasticity modulus of this material were very close to human bones[25]. Pin-on-disk test was adopted. The specimens of the tests are shown in Fig. 12.

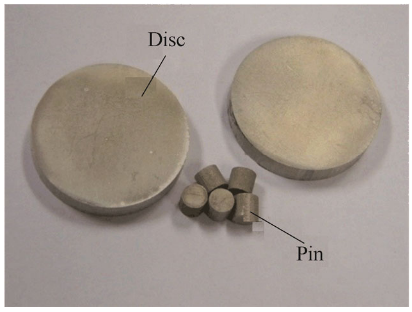

Fig. 12. Specimens made of magnesium alloy

In this test, the emphasis was focused on the wear performances, such as wear scars and wear debris. For comparison, one-way tests on a pin-on-disk rig were also conducted.

The consistency of different stations was carried out. Referring to the similar bio-experiments[26], glass slides and titanium alloy plugs were adopted as the lower and the upper specimens, respectively.

The introductions of the six experiments with four different materials are shown in Table 1 and Table 2.

Table 1. Names and materials of the tests

Test No.	Test Name	Material
1	Multi-directional friction	Magnesium alloys
2	Multi-directional friction	Magnesium alloys
3	Consistency	Titanium alloy
4	Consistency	Glass
5	Variable load	Knee cartilage
6	Variable load	Titanium

Table 2. Parameters of the tests

Test No.	Size /mm	Load /N	Stroke /mm	Velocity /(mm • s^{-1})	Time /s
1	Pin($\Phi\times H$): 5×4.3	20	5	10	2000
2	Disc($\Phi\times H$): 30.5×4.3	20	5	10	2000
3	Pin($\Phi\times H$): 7×3	18	6	6	2000
4	Disk($L\times W$) : 25×10	18	6	6	2000
5	Pin($\Phi\times H$): 6×2.5	16 18 20	10	6	120
6	Disc($\Phi\times H$): 30×4	16 18 20	10	6	120

3.1 Multi-directional friction tracks

The counter-face of lower specimen was examined after the test with SEM(HITACHI SU-8010). The results of the tests are shown in Fig. 13.

Being different from the initial surface shown in Fig. 13(a), some grinding cracks generated by burnishing and scratching are observed on the worn surfaces shown in Figs. 13(b)–(c).

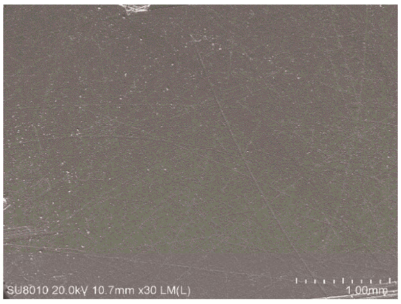

(a) Initial surface of the disc(SEM)

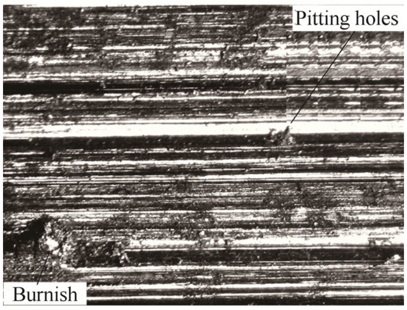

(b) Grinding cracks from a normal pin-on-disk tester(×40)

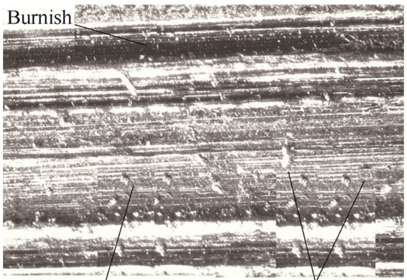

(c) Grinding cracks from the multi-station tribo-tester(×40)

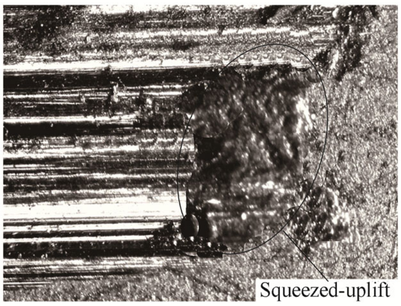

(d) Debris accumulation from a normal pin-on-disk tester(×40)

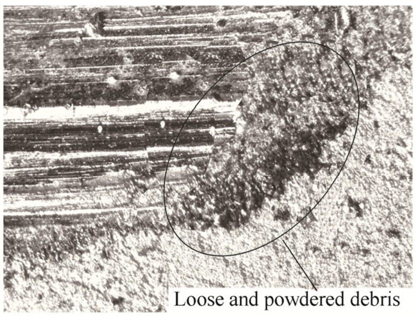

(e) Debris accumulation from the multi-station tribo-tester(×40)

Fig. 13. SEM images of the validation experiments

Comparatively, more deep and uniform grooves are founded on the worn surfaces of one-way friction tests as shown in Fig. 13(b). Due to the large radius of the whole friction tracks and the limited visible fields, it is difficult to identify the geographical differences of the tracks produced in the multi-directional and one-way friction tests.

Multi-directional friction produced scratches because of the contact points existing in one surface, and the scratches were crossing and overlapping. In this process, grooves were produced and polished alternatively. Therefore, no deep grooves can be maintained except for the last cycles. This explanation agrees with the observation in Fig. 13(c).

Another evidence for the differences of the two concerned friction motions can be found in their by-products, wear debris. The two typical images of the two kinds of wear debris are shown in Figs. 13(d)–(e). For one-way friction, most wear debris are pushed by the pin specimens and eventually accumulated as deposits, as shown in Fig. 13(d). Conversely, no collection of wear debris is founded in the multi-directional friction, as shown in Fig. 13(e). Actually, some small, loose and powder wear particles are found scatted around the end of the track. Basically, One-way friction causes wear debris by similar surface morphological contacts, while multi-directional friction generated wear debris by non-uniform contact surfaces. In addition, the grinding cracks are cross-linked and multi-directional[27–29].

Comparing the optical micrographs of the grinding cracks, as shown in Fig. 13(b) and Fig. 13(c), both of them have many longitudinal scratches, but the grinding cracks from the multi-station tribo-test system are much shallower. Meanwhile, there are lots of pitting holes, while the cracks are smoother. Comparing the images in Fig. 13(d) and Fig. 13(e), there is more wear debris in the end of grinding cracks in the developed tribo-tester. The reason is that the combination of reciprocating and rotation is multi-directional, leading to the increases of wear rates and the reduction of surface roughness.

3.2 Consistency of four stations

With the four highly consistent samples, the consistency of four stations was examined with synchronous experiments. The average loads and friction coefficients were compared among these experiments and the mean Standard Deviation(SD) index was adopted for evaluation. The specimens are shown in Fig. 14.

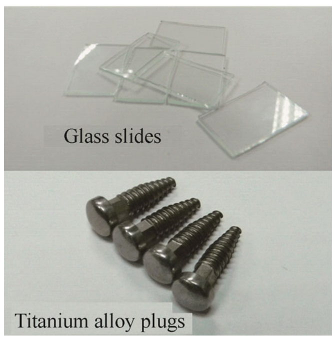

Fig. 14. Glass slide and titanium alloy plug

The tests' results are shown in Fig. 15. The average normal force of station 4 is 17.997 N with a maximal Standard Deviation, which is only 0.2036, and the deviation is 1.13%. For the friction coefficient, the station 2 has a maximal Standard Deviation, which is only 0.0054, and the deviation is 10.26%.

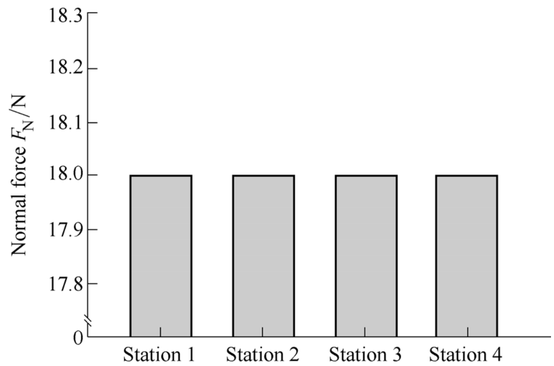

(a) Variation in the normal force

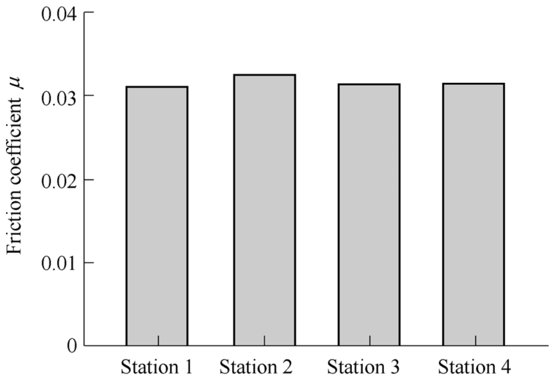

(b) Friction coefficient

Fig. 15. Results of the glass slide and titanium alloy plug tests

For each station, the precision of both normal load and friction coefficient meets the requirements, i.e., the deviation is within ±5%, which accords with ISO 14243−1: 2009.

3.3 Variable loading ability

The cartilage surfaces of knees from a sheep are chosen as the upper specimen, as shown in Fig. 16.

The normal loads were changed from the input value automatically, without manual operations on the tribo-test system. The curves of normal loads, friction forces and the friction coefficients are shown in Fig. 17, respectively.

The figure shows that the multi-station tribo-test system can automatically change loads, and has an accurate measurement of subtle changes in the friction coefficient.

4 Conclusions

(1) Aiming at the comprehensive evaluation of bio-tribological performances of prosthetic materials applied in vitro, a new four-station tribo-test system is presented, with particular consideration on the existing test limitation and validations by four different materials.

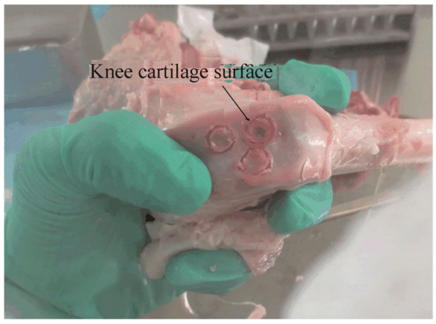

(a) Cartilage surfaces of knees from a sheep

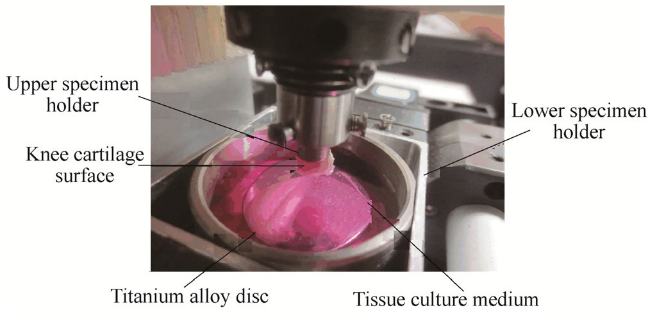

(b) Clamping of the specimens

Fig. 16. Knee cartilage and titanium test

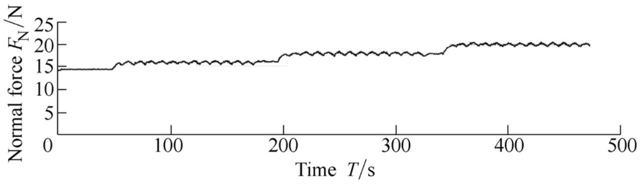

(a) Curves of normal force

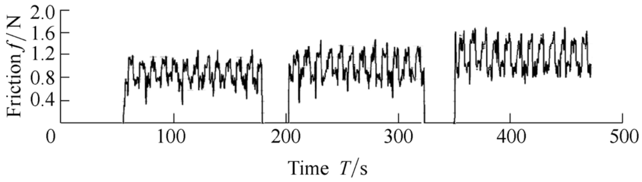

(b) Curves of friction force

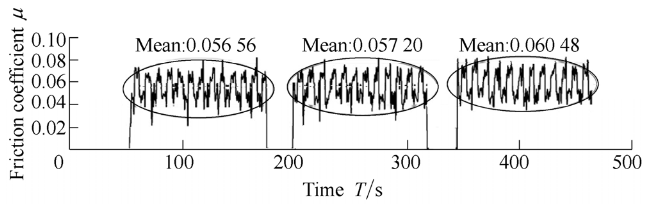

(c) Curves of friction coefficient

Fig. 17. Results of the knee cartilage and titanium test

(2) Comparability and repeatability of a tribo-test are ensured by designing an independent multi-station structure. The multi-station can provides synthetic and independent experiments simultaneously.

(3) The multi-directional motions between the specimens and the sliding friction are accomplished, where the cross-linked scratches between tribo-pairs of human joints can be simulated by different materials. The friction tracks can be designed by varying reciprocating and rotating speeds. And their precisions meet the requirements described in ISO 14243-1: 2009 very well.

(4) The normal loading forces can be changed

automatically by the proposed variable loading system, which facilitates the simulation of the gaits during walking.

(5) The variable frictional tracks can produce different wear debris compared with one-directional tracks, and the accuracy of loading and friction force is within $\pm 5\%$.

References

[1] RIEKER C B. Tribology in total hip arthroplasty: historical development and future trends[C]//*The 2nd World Tribology C*onference, Vienna, 2001: 750.

[2] DOWSON D. Bio-tribology[J]. *Faraday Discussions,* 2012, 156(1): 9–30.

[3] KUSTER M S, WOOD G A, STACHOWIAK K S, et al. Joint bad considerations in total knee replacement[J]. *Journal of Bone and Joint Surgery*, 1997, 79(1): 109–113.

[4] MATTEI L, DI P F, PICCIGALLO B, et al. Lubrication and wear modelling of artificial hip joints: A review[J]. *Tribology International*, 2011, 44(5): 532–549.

[5] DAMM P, DYMKE J, ACKERMANN R, et al. Friction in total hip joint prosthesis measured in vivo during walking[J]. *PLoS ONE*, 2013, 8(11): 42.

[6] BERGMANN G, DEURETZBACHER G, HELLER M, et al. Hip contact forces and gait patterns from routine activities[J]. *Journal of Biomechanics*, 2001, 34(7): 859–871.

[7] BERGMANN G, GRAICHEN F, ROHLMANN A. Hip joint loading during walking and running, measured in two patients[J]. *Journal of Biomechanics*, 1993, 26(8): 969–990.

[8] DAMM P, GRAICHEN F, ROHLMANN A, et al. Total hip joint prosthesis for in vivo measurement of forces and moments[J]. *Medical Engineering & Physics*, 2010, 32(1): 95–100.

[9] PROTOPOPOV B V. Some features of tribosystem standardization[J]. *Wear of Material, AMSE*, 1991: 659–660.

[10] KENNETH C L. Seventy years of research on wear[J]. *ASME TRIB*, 1990, 1: 111–128.

[11] BOWLAND P, INGHAM E, JENNINGS L, et al. Review of the biomechanics and biotribology of osteochondral grafts used for surgical interventions in the knee[J]. *Proceedings of the Institution of Mechanical Engineers, Part H: Journal of Engineering in Medicine*, 2015, 229(12): 879–888.

[12] JIN Z M, STONE M, INGHAM E, et al. Biotribology[J]. *Current Orthopaedics*, 2006, 20(1): 32–40.

[13] FAN Yongwei, HUA Zikai, WU Yitian, et al. A new biological implant material wear test machine[J]. *Journal of Shanghai University(Natural Science)*, 2014, 20(4): 397–403. (in Chinese).

[14] STEWART T D, TIPPER J L, INSLEY G, et al. Long-term wear of ceramic matrix composite materials for hip prostheses under severe swing phase micro separation[J]. *Journal of Biomedical Materials Research Part B*, 2003, 66(2): 567–573.

[15] HUA Zikai, FAN Yongwei, ZHANG Huanhuan, et al. Research and development of multi-directional wear testing apparatus for artificial joint materials[J]. *Journal of Hebei University of Science and Technology*, 2014, 35(1): 6–10. (in Chinese).

[16] SAIKKO V, AHLROOS T. Phospholipids as boundary lubricants in wear tests of prosthetic joint materials[J]. *Wear*, 1997, 207(1): 86–91.

[17] TWORZYDLO W W, HAMZEH O N, ZATON W, et al. Friction-induced oscillations of a pin-on-disk slider: analytical and experimental studies[J]. *Wear*, 1999, 236(1): 9–23.

[18] CHARNLEY J. Wear of plastics materials in hip-joint[J]. *Plastics and Rubber*, 1976, 1(2): 59–63.

[19] SAIKKO V. A multidirectional motion pin-on-disk wear test method for prosthetic joint materials[J]. *Journal of Biomedical Materials Research*, 1998, 41(1): 58–64.

[20] KORDUBA L A, WANG A. The effect of cross-shear on the wear of virgin and highly-crosslinked polyethylene[J]. *Wear*, 2011, 271(9): 1220–1223.

[21] CALONIUS O, SAIKKO V. Analysis of relative motion between femoral head and acetabular cup and advances in computation of the wear factor for the prosthetic hip joint[J]. *Acta Polytechnica*, 2003, 43(4): 43–54.

[22] LAURENT M P, JOHNSON T S, YAO J Q, et al. In vitro lateral versus medial wear of a knee prosthesis[J]. *Wear*, 2003, 255(7): 1101–1106.

[23] SAIKKO V. A multidirectional motion pin-on-disk wear test method for prosthetic joint materials[J]. *Journal of Biomedical Materials Research*, 1998, 41(1): 58–64.

[24] ZHAI Wenjie, WANG Chuang. The development of friction tester admitting of changing-direction grinding[J]. *Machine Design and Research*, 2003, 16(4): 60–61. (in Chinese).

[25] STAIGER M P, PIETAK A M, HUADMA J, et al. Magnesium and it alloys as orthopedic biomaterials: a review[J]. *Biomaterials*, 2006, 27(9): 1728–1734.

[26] ZHANG Yongquan, WANG Junlin, WANG Pan, et al. Low elastic modulus contributes to the osteointegration of titanium alloy plug[J]. *Journal of Biomedical Materials Research Part B: Applied Biomaterials*, 2013, 101(4): 584–590.

[27] HOLLEY K G, FURMAN B D, BABALOLA O M, et al. Impingement of acetabular cups in a hip simulator-comparison of highly cross-linked and conventional polyethylene[J]. *The Journal of Arthroplasty*, 2005, 20: 77–86.

[28] AFFATATO S, BERSAGLIA G, ROCCHI M, et al. Wear behavior of cross-linked polyethylene assessed in vitro under severe conditions[J]. *Biomaterials*, 2005, 26(16): 3259–3267.

[29] KYOMOTO M, MORO T, KONNO T, et al. Effects of photo-induced graft polymerization of 2-methacryloyloxyethyl phosphor choline on physical properties of cross-linked polyethylene in artificial hip joints[J]. *Materials in Medicine*, 2007, 18(9): 1809–1815.

Biographical notes

WU Tonghai, born in 1976, is currently a professor at *Theory of Lubrication and Bearing Institute, Key Laboratory for Modern Design and Rotor-Bearing System of Ministry of Education, Xi'an Jiaotong University, China*. He obtained his PhD degree from *Xi'an Jiaotong University, China*, in 2006. His research interests include tribology system and intelligent monitoring.
Tel: +86-29-82669161; E-mail: wt-h@163.com

DU Ying, born in 1989, is currently a PhD candidate at *Theory of Lubrication and Bearing Institute, Key Laboratory for Modern Design and Rotor-Bearing System of Ministry of Education, Xi'an Jiaotong University, China*. She received her master degree from *Xi'an Jiaotong University, China*, in 2013.
E-mail: duying2007@msn.com

LI Yang, born in 1989, is currently a graduate candidate and received his master degree from *Theory of Lubrication and Bearing Institute, Xi'an Jiaotong University, China*, in 2015.
E-mail: lneyang@163.com

WANG Shuo, born in 1990, is currently a master candidate at *Theory of Lubrication and Bearing Institute, Key Laboratory for Modern Design and Rotor-Bearing System of Ministry of Education, Xi'an Jiaotong University, China*.
E-mail: wstyxjtu@163.com

ZHANG Zhinan, born in 1978, is currently a research assistant at *School of Mechanical Engineering, Shanghai Jiao Tong University, China*. He received his PhD degree from *Shanghai Jiao Tong University, China*, in 2011. His research interests include design theory and tribology design.
E-mail: zhinanz@sjtu.edu.cn